

Ground state topology of a four-terminal superconducting double quantum dot

Lev Teshler¹, Hannes Weisbrich¹, Raffael L. Klees², Gianluca Rastelli³ and Wolfgang Belzig^{1*}

¹ Fachbereich Physik, Universität Konstanz, Universitätsstraße 40, 78457 Konstanz, Germany

² Institut für Theoretische Physik und Astrophysik, Julius-Maximilians-Universität Würzburg, Am Hubland, 97074 Würzburg, Germany

³ Pitaevskii Center on Bose-Einstein Condensation, CNR-INO and Dipartimento di Fisica dell'Università di Trento, Via Sommarive 14, 38123 Trento, Italy

* wolfgang.belzig@uni-konstanz.de

April 25, 2023

Abstract

In recent years, various classes of systems were proposed to realize topological states of matter. One of them are multiterminal Josephson junctions where topological Andreev bound states are constructed in the synthetic space of superconducting phases. Crucially, the topology in these systems results in a quantized transconductance between two of its terminals comparable to the quantum Hall effect. In this work, we study a double quantum dot with four superconducting terminals and show that it has an experimentally accessible topological regime in which the non-trivial topology can be measured. We also include Coulomb repulsion between electrons which is usually present in experiments and show how the topological region can be maximized in parameter space.

Contents

1	Introduction	2
2	Main results	3
2.1	Single-particle Hamiltonian	3
2.2	Andreev bound states and topology	4
2.3	Many-body Hamiltonian	5
2.4	Ground state spin	7
2.5	Enhancement of the topological phases	7
3	Conclusion	9
A	Full Dyson equation and self-energy of the DQD	10
B	Calculation of the many-body Hamiltonian	10
C	Effect of different parameters on the topological phase diagram	11
	References	12

1 Introduction

Topology and related concepts is a central theme of modern solid state physics by explaining ultimately the nature of quantized phenomena. The discovery of the quantum Hall effect [1] and its quantized conductance which can be explained in terms of the 2D topological invariant of the first Chern number [2] started an ongoing search for novel topological materials for the past decades. It brought a unique understanding of topological insulators that are insulating in the bulk but have conducting edge states [3]. Moreover, the study of topological superconductors [4] started the concept of Majorana zero-energy modes that promises topologically protected quantum computing [5–8] on the basis of their non-Abelian braiding statistics.

More recently, synthetic topological matter is intensely studied. Here the topology is constructed in internal degrees of freedom and thus allows for a better control of the topological properties. Prime examples are topological photonics [9, 10], topological driven Floquet systems [11] and topological electrical circuits [12]. This idea was also successfully transferred to multiterminal Josephson junctions [13–26] or topological superconducting circuits [27–29], where topological Andreev bound states are constructed in the space of the superconducting phases. With such approach the dimensionality of the phase space and the related topology is in principle unlimited and only depends on the number of superconducting terminals [30–32]. The non-trivial topology of the bound states results in a quantized transconductance [13] in units of $4e^2/h$ when applying voltages to the superconducting terminals. In general, these Andreev bound states can be also experimentally accessed by coherent microwave drive [33–35] and spectroscopy [36, 37]. Despite the fact that there are already experimental realizations of multiterminal Josephson junction devices [38–41], an evidence of a non-trivial topology in such system is still lacking. Although there are numerous proposals regarding topological multiterminal Josephson junctions these systems remain experimentally challenging due to the need of specific scattering regions in between the terminals [14–17]. An alternative approach is based on the coupling of quantum dots to superconducting leads [21, 22, 42] that in principle leads to a better control of the processes within the multiterminal Josephson junction. However the existing proposals still require an advanced coupling between the superconducting terminals that limits the feasibility of such proposals. Here we study a system with a double quantum dot that only requires a coupling between a double quantum and four superconducting terminals that realizes topological Andreev bound states. Similar systems based on a carbon nanotube with a double quantum dot coupled to two terminals [43, 44] or a single quantum dot coupled to three terminals [45] were already realized experimentally and, thus, this proposal should be in the reach of current experimental devices to finally observe topological Andreev bound states and the related quantized transconductance.

We begin by deriving the effective low energy Hamiltonian of the system in the single-particle picture in section 2.1 and analyzing the topology of its Andreev bound states in section 2.2. In section 2.3 we switch to the many-body picture that allows to include Coulomb interaction between electrons. Finally, in section 2.4 we look at the total spin of the many-body ground state and discuss the parameter regimes for which the non-trivial topology can be detected.

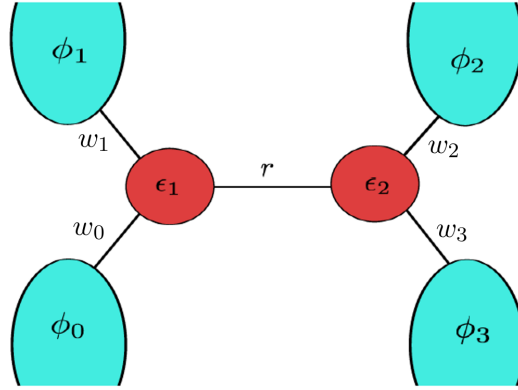


Figure 1: The system consists of a double quantum dot with inter-dot coupling r and four superconductors with respective superconducting phases φ_j which are coupled to the quantum dots via w_j for $j = 0, 1, 2, 3$. The first two superconductors are coupled to the first quantum dot and the last two superconductors are coupled to the second quantum dot.

2 Main results

2.1 Single-particle Hamiltonian

The considered system is a double quantum dot (DQD), where each quantum dot is coupled to two superconductors (SCs) via couplings w_j (see Figure 1). In the absence of any interaction between the quantum dots it describes two isolated Josephson junctions (JJs) whose Andreev bound states (ABS) have energies $\pm E_1(\varphi_1 - \varphi_0)$ and $\pm E_2(\varphi_3 - \varphi_2)$. However, for finite interaction r between the quantum dots the ABS hybridize and, thus, depend on all SC phases. This hybridization is crucial for the non-trivial topology of the bound states in the SC phase space as will be discussed below.

The Hamiltonian of the DQD system can be written in the basis $\vec{d}^\dagger = (d_{1,\uparrow}^\dagger, d_{1,\downarrow}, d_{2,\uparrow}^\dagger, d_{2,\downarrow})$ of the dot-spin space as $H_D = \vec{d}^\dagger \tilde{H}_D \vec{d}$ with the matrix Hamiltonian

$$\tilde{H}_D = \begin{pmatrix} \varepsilon_1 & r \\ r & \varepsilon_2 \end{pmatrix} \otimes \tau_3. \quad (1)$$

Here, $\varepsilon_1, \varepsilon_2$ are the on-site energies of the dots, r the inter-dot coupling and τ_j the Pauli matrices.

The four superconductors, in turn, are described by $H_S = \sum_k \tilde{c}_k^\dagger \tilde{H}_{S,k} \tilde{c}_k$ with $\tilde{c}_k^\dagger = (c_{0k\uparrow}^\dagger, c_{0-k\downarrow}, \dots, c_{3k\uparrow}^\dagger, c_{3-k\downarrow})$ with matrix Hamiltonian $\tilde{H}_{S,k} = \text{diag}(\tilde{H}_{S,0k}, \tilde{H}_{S,1k}, \tilde{H}_{S,2k}, \tilde{H}_{S,3k})$, where each block on the diagonal,

$$\tilde{H}_{S,jk} = \xi_{jk} \tau_3 + \Delta_j e^{i\varphi_j \tau_3} \tau_1, \quad (2)$$

describes a BCS superconductor with superconducting phase φ_j , gap Δ_j and normal state dispersion ξ_{jk} . In the following, we choose a gauge such that $\varphi_0 = 0$.

To describe the interactions between the DQD and the SC terminals, we introduce $H_{DS} = \sum_k$

$(\tilde{d}^\dagger \tilde{V}_{DS} \tilde{c}_k + \text{H.c.})$ with

$$\tilde{V}_{DS} = \begin{pmatrix} w_0 & w_1 & 0 & 0 \\ 0 & 0 & w_2 & w_3 \end{pmatrix} \otimes \tau_3, \quad (3)$$

where w_j is the coupling of terminal j to the quantum dots.

The Dyson equation for the total system (see Appendix A) can be solved for the dressed Green's function (GF) of the DQD, $\tilde{G}_{DD} = \tilde{g}_{DD} + \tilde{g}_{DD} \tilde{\Sigma}_{DD} \tilde{G}_{DD}$, where we identified the self-energy $\tilde{\Sigma}_{DD} = \tilde{V}_{DS} \tilde{g}_{SS} \tilde{V}_{DS}^\dagger$ that describes the proximity coupling of the DQD to the SCs. Here, \tilde{G}_i and \tilde{g}_i are the dressed and bare matrix GF, respectively, and $i = D, S$ stands for the DQD and SC system, respectively. To calculate the self-energy, we need the bare GF of the SC system, which we obtain by inverting its Hamiltonian as $\tilde{g}_{SS}(E) = (E - \tilde{H}_S)^{-1}$.

Assuming the energy E to be much smaller than the superconducting gaps Δ_j of the superconductors (low energy limit), we obtain the matrix GF $\tilde{g}_{SS} = \text{diag}(\tilde{g}_{S,0}, \tilde{g}_{S,1}, \tilde{g}_{S,2}, \tilde{g}_{S,3})$ with

$$\tilde{g}_{S,j}(E) = -\pi N_0 \frac{E + \Delta_j e^{i\varphi_j \tau_3} \tau_1}{\sqrt{\Delta_j^2 - E^2}} \xrightarrow{E \rightarrow 0} -\pi N_0 e^{i\varphi_j \tau_3} \tau_1 \quad (4)$$

for $j = 0, 1, 2, 3$. A detailed calculation of this can be found in [22].

Calculating the self-energy (Eq. (A3)) and adding it to the Hamiltonian in Eq. (1) we obtain the effective low energy Hamiltonian of the DQD in the spinor basis $\tilde{d}^\dagger = (d_{1,\uparrow}^\dagger, d_{1,\downarrow}^\dagger, d_{2,\uparrow}^\dagger, d_{2,\downarrow}^\dagger)$,

$$\tilde{H}_{D,\text{eff}} = \begin{pmatrix} \varepsilon_1 & \Gamma_0 + \Gamma_1 e^{i\varphi_1} & r & 0 \\ \Gamma_0 + \Gamma_1 e^{-i\varphi_1} & -\varepsilon_1 & 0 & -r \\ r & 0 & \varepsilon_2 & \Gamma_2 e^{i\varphi_2} + \Gamma_3 e^{i\varphi_3} \\ 0 & -r & \Gamma_2 e^{-i\varphi_2} + \Gamma_3 e^{-i\varphi_3} & -\varepsilon_2 \end{pmatrix}, \quad (5)$$

where $\Gamma_j = \pi N_0 w_j^2$ are the effective couplings between the quantum dots and the superconducting terminals. The self-energy terms can be interpreted as transitions of Cooper pairs between superconductors and dots with phase-dependent amplitudes that we are going to denote $\Gamma_{01} = \Gamma_0 + \Gamma_1 e^{i\varphi_1}$ and $\Gamma_{23} = \Gamma_2 e^{i\varphi_2} + \Gamma_3 e^{i\varphi_3}$ for later convenience.

2.2 Andreev bound states and topology

The DQD system has four ABS (see Figure 2), as follows from the 4×4 low energy Hamiltonian in Eq. (5). Their energies can be calculated by imposing $\det(E - H_{D,\text{eff}}) = 0$ which leads to a quartic equation with solutions,

$$E_{1,2}^2 = b/2 \pm \sqrt{(b/2)^2 - c}, \quad (6)$$

where

$$\begin{aligned} b &= \varepsilon_1^2 + \varepsilon_2^2 + 2r^2 + |\Gamma_{01}|^2 + |\Gamma_{23}|^2, \\ c &= r^4 + \varepsilon_1^2 \varepsilon_2^2 + \varepsilon_1^2 |\Gamma_{23}|^2 + \varepsilon_2^2 |\Gamma_{01}|^2 + |\Gamma_{01}|^2 |\Gamma_{23}|^2 + r^2 (\Gamma_{01} \Gamma_{23}^* + \Gamma_{23} \Gamma_{01}^* - 2\varepsilon_1 \varepsilon_2). \end{aligned} \quad (7)$$

The four eigenenergies come in symmetric pairs $\pm E_{1,2}$ as a result of particle-hole (PH) symmetry of the system. For $r = 0$, the system decouples into two independent Josephson junctions with eigenenergies $E_1 = \sqrt{\varepsilon_1^2 + \Gamma_{01}^2}$ and $E_2 = \sqrt{\varepsilon_2^2 + \Gamma_{23}^2}$. The isolated ABS each depend only on one phase difference and are, hence, topologically trivial.

Generically, the Hamiltonian in Eq. (5) and its eigenstates depend on three phase differences which serve as synthetic dimensions for the topology. A non-trivial topology in terms of the Chern

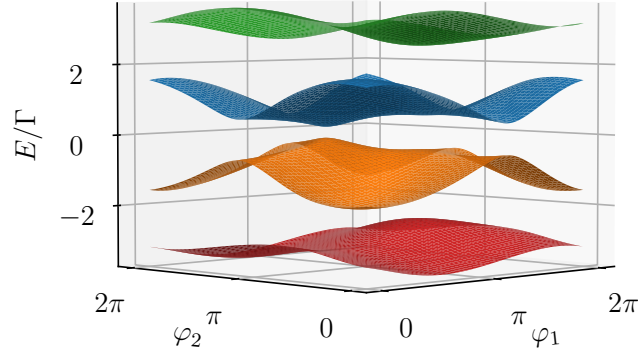


Figure 2: All four energy bands of the two-dot system for $\varphi_3 = \pi/2$, $\varepsilon_i = \Gamma_i = \Gamma$ and $r = 1.5\Gamma$. PH symmetry results in a symmetric spectrum. In the ground state only the red and orange energy bands with negative energy are occupied.

number C_{12} with respect to the superconducting phases φ_1 and φ_2 leads to a quantized transconductance $G_{12} = (-4e^2/h)C_{12}$ between terminals 1 and 2 when applying incommensurate voltages to those two terminals [13]. Here, e is the elementary charge and h the Planck constant.

With $|n\rangle$ denoting the phase-dependent eigenstates sorted by $n = 1, 2, 3, 4$ in order of increasing energy, the Berry Connection of the n th eigenstate is defined as $a_\alpha^{(n)} = i \langle n | \partial_\alpha | n \rangle$ where we use $\partial_\alpha = \partial / \partial \varphi_\alpha$. From this we can define the Berry curvature $f_{\alpha\beta}^{(n)} = \partial_\alpha a_\beta^{(n)} - \partial_\beta a_\alpha^{(n)}$ of the n th eigenstate with respect to the phases φ_α and φ_β . Finally, the corresponding Chern number of the n th eigenstate is defined as

$$c_{\alpha\beta}^{(n)} = \frac{1}{2\pi} \int_0^{2\pi} \int_0^{2\pi} f_{\alpha\beta}^{(n)} d\varphi_\alpha d\varphi_\beta, \quad (8)$$

which is quantized to integer values. Since we are in the single-particle picture, in the ground state (GS) all states below the Fermi energy ($E_F = 0$) are occupied. Because of PH symmetry of the Hamiltonian, two of the four eigenenergies are negative, meaning that the ground state Chern number is given by the sum over the two lowest eigenstates,

$$C_{12}^{\text{GS}} = c_{12}^{(1)} + c_{12}^{(2)}. \quad (9)$$

Changing the GS Chern number requires a closing of the gap between two energy bands at zero energy, so called Weyl points, which change the value of the Chern number by ± 1 . Figures 3b and 3c show such Weyl points in φ_1 - φ_2 space. The two spectra are obtained for parameters corresponding to the red and blue dots in Figure 3a, respectively, which lie on boundaries between different topological phases. Figure 3a also demonstrates that non-trivial topological phases (with non-zero Chern number) exist when the inter-dot coupling r is comparable to the effective couplings $\Gamma_i = \Gamma$ between the SCs and quantum dots.

2.3 Many-body Hamiltonian

The Hamiltonian in Eq. (5) is written in the basis \tilde{d}^\dagger of single-particle creation and annihilation operators. Thus, treatment in the single-particle picture is sufficient. To describe the Zeeman splitting in a magnetic field B and the Coulomb repulsion between two electrons, however, we

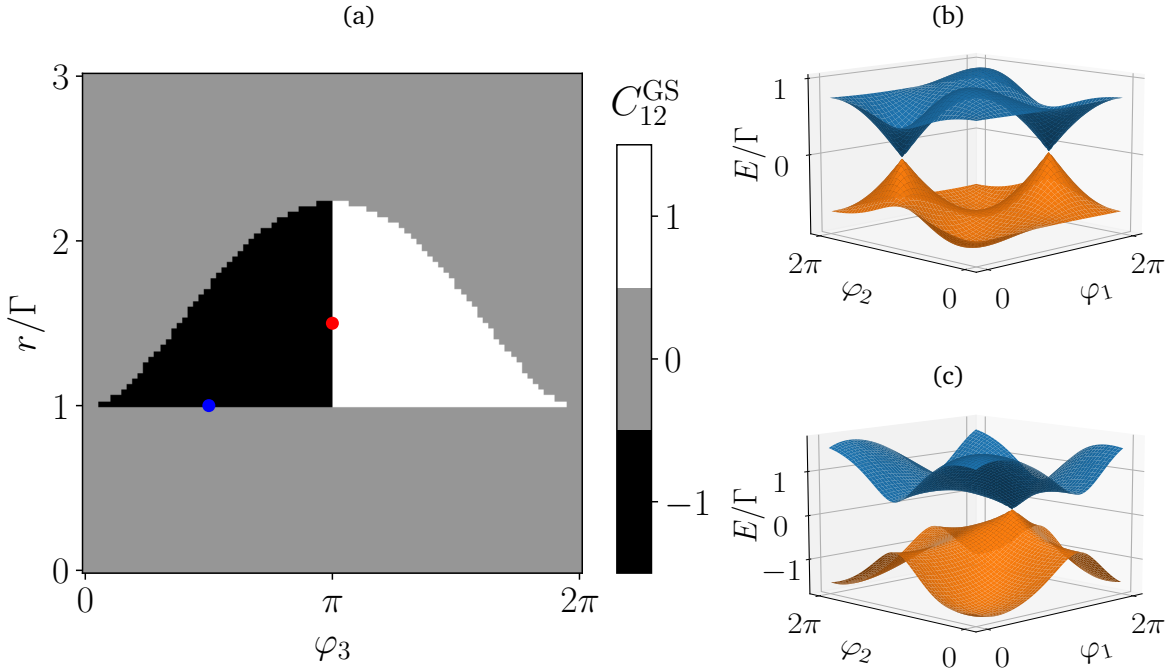


Figure 3: (a) Topological phase diagram: First Chern number as a function of r and φ_3 for $\Gamma_i = \Gamma = \varepsilon_i$. (b) Spectrum of the ground state and first excited state for $\varphi_3 = \pi$ and $r = 1.5\Gamma$ (red point). (c) Same spectrum for $\varphi_3 = \pi/2$ and $r = \Gamma$ (blue point).

extend our Hamiltonian to

$$H_D = H_{D,\text{eff}} + \frac{B}{2}(n_{1\uparrow} + n_{2\uparrow} - n_{1\downarrow} - n_{2\downarrow}) + U_C(n_{1\uparrow}n_{1\downarrow} + n_{2\uparrow}n_{2\downarrow}), \quad (10)$$

where $n_{i\sigma} = d_{i\sigma}^\dagger d_{i\sigma}$ are the particle number operators for electrons with spin σ on dot i and U_C is the Coulomb energy of an electron pair on the same dot. We only include Coulomb interaction between electrons on the same dot (intra-dot), since the inter-dot Coulomb interaction should be significantly weaker and, if included, has a very similar effect on the topological phase diagram.

Hamiltonian 10 can not be expressed in the single-particle basis \tilde{d}^\dagger . We, therefore, need to choose an appropriate basis of many-body states. In the many-body picture, in the GS only the lowest energy state is occupied, so the GS Chern number is just the Chern number of the lowest energy eigenstate.

First, let us note that each of the two quantum dots can host zero, one or two electrons, in the latter case with opposite spin due to the Pauli principle. The possible single quantum dot states are, thus, $|0\rangle, |\uparrow\rangle, |\downarrow\rangle, |\uparrow\downarrow\rangle$. For the double quantum dot, we have $2^4 = 16$ possible basis states, which we denote as $|\alpha, \beta\rangle$, if dot 1 is in state $|\alpha\rangle$ and dot 2 in state $|\beta\rangle$.

We would like to note, that the Hamiltonian in Eq.(10) contains only terms with an even number (two or four) of fermionic operators and, thus, conserves the fermionic parity. We can, thus, divide the many-body states into two sectors with even and odd numbers of electrons. Conservation of the total spin allows us to subdivide the even parity sector into a singlet (spin 0) and triplet (spin 1) sector, while the odd parity sector corresponds to a doublet with spin 1/2. We shall look at the 3 spin sectors separately.

For the singlet sector, we can choose the basis $\{|0, 0\rangle, (|\uparrow, \downarrow\rangle - |\downarrow, \uparrow\rangle)/\sqrt{2}, |\uparrow\downarrow, 0\rangle, |0, \uparrow\downarrow\rangle, |\uparrow\downarrow, \uparrow\downarrow\rangle\}$ and obtain the matrix Hamiltonian

$$\tilde{H}_D^{\text{singlet}} = \begin{pmatrix} 0 & 0 & \Gamma_{01}^* & \Gamma_{23}^* & 0 \\ 0 & \varepsilon_1 + \varepsilon_2 & \sqrt{2}r & \sqrt{2}r & 0 \\ \Gamma_{01} & \sqrt{2}r & 2\varepsilon_1 + U_C & 0 & \Gamma_{23}^* \\ \Gamma_{23} & \sqrt{2}r & 0 & 2\varepsilon_1 + U_C & \Gamma_{01}^* \\ 0 & 0 & \Gamma_{23} & \Gamma_{01} & 2(\varepsilon_1 + \varepsilon_2) + 2U_C \end{pmatrix}. \quad (11)$$

How the many-body Hamiltonian is calculated is explained in Appendix B. This 5×5 Hamiltonian has five energy levels, one of which is completely phase-independent due to symmetry.

The doublet sector has eight energy levels. As basis we set $|\sigma\pm\rangle = (|\sigma, 0\rangle \pm |0, \sigma\rangle)/\sqrt{2}$ and $|t\sigma\pm\rangle = (|\sigma, \uparrow\downarrow\rangle \pm |\uparrow\downarrow, \sigma\rangle)/\sqrt{2}$ for $\sigma = \uparrow, \downarrow$. Choosing the basis order $|\uparrow\pm\rangle, |t\uparrow\pm\rangle, |\downarrow\pm\rangle, |t\downarrow\pm\rangle$, we obtain the matrix Hamiltonian $\tilde{H}_D^{\text{doublet}} = \sigma_0 \otimes \tilde{H}_{\text{block}} + (B/2)\sigma_3 \otimes \mathbb{1}_{4 \times 4}$, where the last term describes the spin-dependent Zeeman splitting and

$$\tilde{H}_{\text{block}} = \frac{1}{2} \begin{pmatrix} \varepsilon_1 + \varepsilon_2 + 2r & \varepsilon_1 - \varepsilon_2 & \Gamma_{01}^* + \Gamma_{23}^* & \Gamma_{01}^* + \Gamma_{23}^* \\ \varepsilon_1 - \varepsilon_2 & \varepsilon_1 + \varepsilon_2 - 2r & \Gamma_{01}^* + \Gamma_{23}^* & \Gamma_{01}^* + \Gamma_{23}^* \\ \Gamma_{01} + \Gamma_{23} & \Gamma_{01} + \Gamma_{23} & 3\varepsilon_1 + 3\varepsilon_2 - 2r + 2U_C & \varepsilon_2 - \varepsilon_1 \\ \Gamma_{01} + \Gamma_{23} & \Gamma_{01} + \Gamma_{23} & \varepsilon_2 - \varepsilon_1 & 3\varepsilon_1 + 3\varepsilon_2 + 2r + 2U_C \end{pmatrix} \quad (12)$$

is the same for both spin subspaces.

Finally, we can choose $|\uparrow, \uparrow\rangle, (|\uparrow, \downarrow\rangle + |\downarrow, \uparrow\rangle)/\sqrt{2}$ and $|\downarrow, \downarrow\rangle$ as basis of the triplet space. The corresponding Hamiltonian is found to be diagonal with phase-independent eigenenergies $\varepsilon_1 + \varepsilon_2 (\pm B)$. These triplet states are, obviously, topologically trivial and so are the doublet states as well, despite their dependence on SC phases. We will, therefore, focus on the singlet states, as only they can be topologically non-trivial. It is, however, only relevant, as long the singlet GS is the overall GS which is crucial for the observation of a quantized transconductance.

2.4 Ground state spin

To find the relevant conditions under which the system has a potentially topological GS, we identify the spin of the overall GS simply by comparing the ground states of the three spin subspaces. Having already found non-trivial topology in the absence of Coulomb interaction and magnetic fields in section 2.2, we will now look at the effect of these two parameters on the GS spin. Fixing $\varepsilon_i = \Gamma_i = \Gamma$, $r = 1.2\Gamma$ and $\varphi_3 = \pi/2$ (values, for which we previously found non-trivial topology), we plot the spin of the GS in the φ_1 - φ_2 Brillouin zone for different values of U_C and B . This is shown in Figure 4. For weak Coulomb repulsion and magnetic fields, we have a singlet GS (red). For $U_C > 0.5\Gamma$, the doublet GS (blue) gradually takes over the entire BZ. Similarly, with increasing B , the Zeeman splitting of the doublet GS eventually overcomes the singlet GS which is unaffected by B . For strong magnetic fields, the triplet GS (gray) prevails, since it has the strongest Zeeman splitting. We conclude that in order to have a topological GS and exactly quantized transconductance, we have to avoid magnetic fields and minimize the Coulomb repulsion between electrons on the same dot.

2.5 Enhancement of the topological phases

For practical applications it is convenient to make the topological phases as large as possible in parameter space, making the quantized conductance G_{12} more robust against fluctuations in those

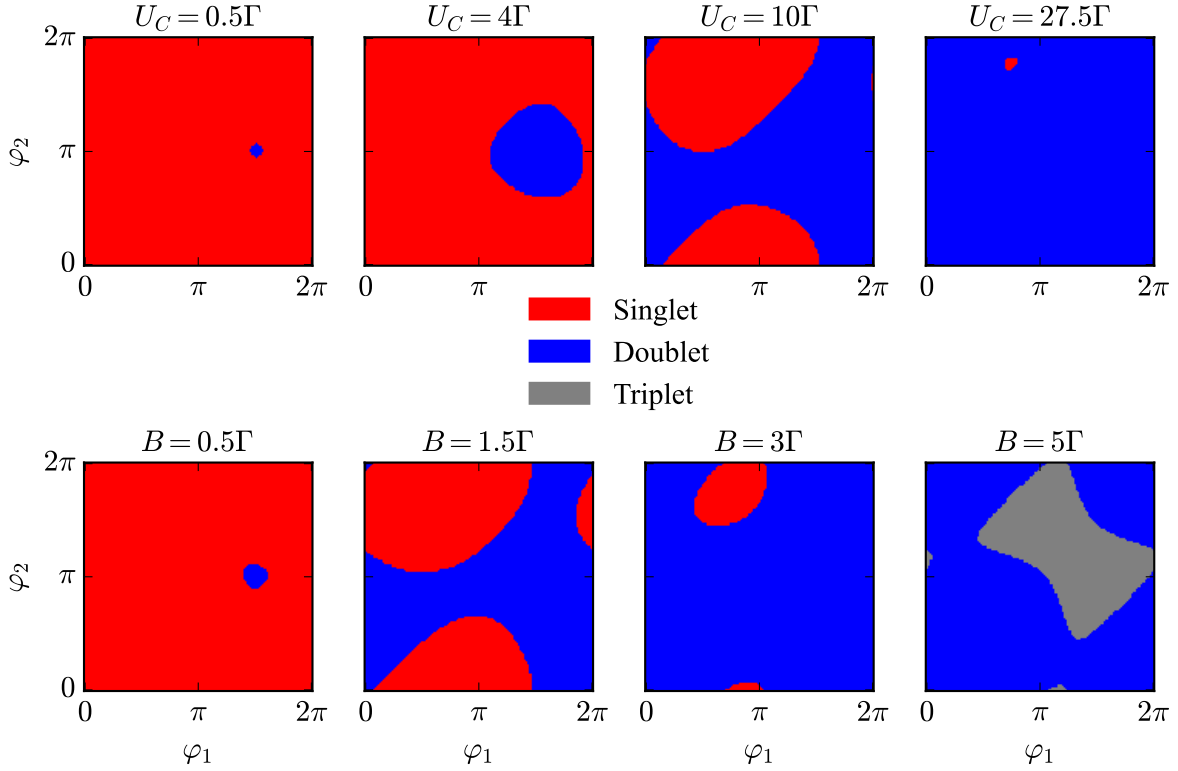


Figure 4: Ground state spin phase diagrams in the φ_1 - φ_2 space for $\varepsilon_i = \Gamma_i = \Gamma$, $r = 1.2\Gamma$ and $\varphi_3 = \pi/2$. In the upper row, the Coulomb interaction U_C is varied, while $B = 0$, in the lower row $U_C = 0$ and the magnetic field B is varied.

parameters. While it is realistic to assume $B \ll \Gamma_i$, it might be problematic to achieve $U_C \ll \Gamma_i$ in experiments. We, thus, assume a finite value $U_C = 0.3\Gamma_0$, which lies in the allowed range $0 < U_C < 0.5\Gamma$ and try to find the values for ε_i and Γ_i that maximize the area of the non-trivial topological phases in φ_3 - r space. The optimal values are equal superconductor couplings $\Gamma_i = \Gamma$ and equal dot energies $\varepsilon_i = \varepsilon < \Gamma$. The topological phase diagrams for other parameter settings can be seen in Appendix C. In fact, reducing ε stretches the phases in r direction, while increasing U_C has the opposite effect. If we recall that $r \ll \Gamma$ corresponds to two decoupled non-topological systems, it becomes clear that this case should be avoided. Figure 5 shows the phase diagram for $U_C = 0.3\Gamma$, $\varepsilon = \Gamma$ and $\varepsilon = 0.3\Gamma$, respectively. For reduced ε , the singlet GS is still the overall GS. There is a clear enhancement of the topological phase by reducing the energy ε of the quantum dots while $U_C \neq 0$. As a result of this enhancement a non-zero Chern number can be achieved with much smaller inter-dot coupling r .

Further reduction of ε extends the topological phase into the region of even smaller r (see Figure 7(d) in Appendix C), at least mathematically. Physically, however, a finite coupling $r \simeq \Gamma$ is required to observe the topology, as explained above. But in principle, setting the energy ε of the quantum dots equal to zero, which is the Fermi energy E_F of the superconductors, is optimal.

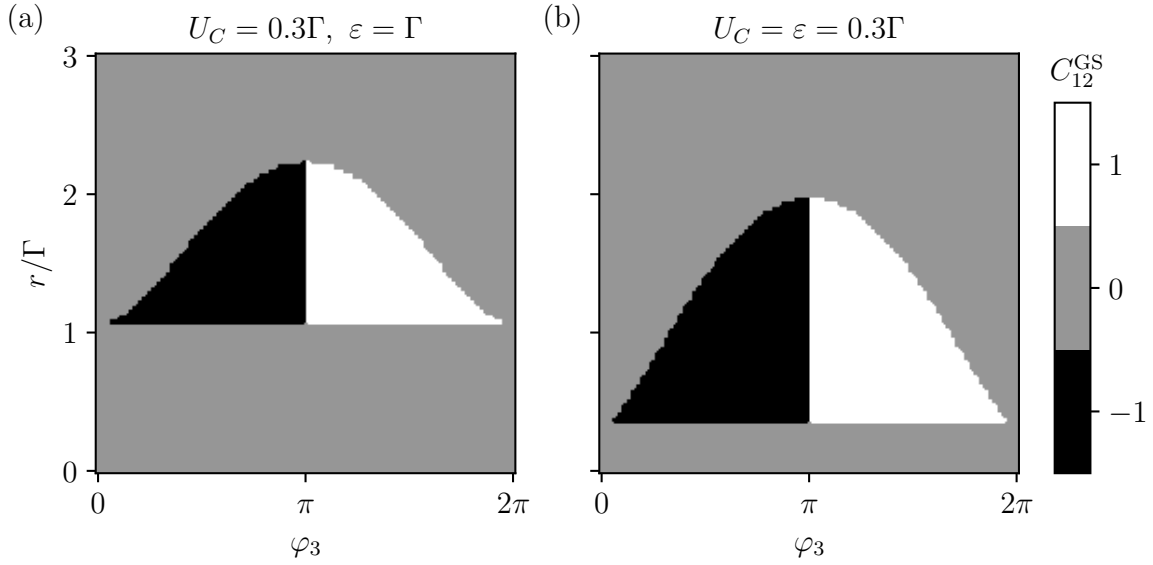


Figure 5: Phase diagram of the ground state with the Chern number C_{12} as a function of φ_3 and r (a) for equal couplings $\Gamma_i = \Gamma$, $U_C = 0.3\Gamma$ and equal dot energies $\varepsilon = \Gamma$ and (b) for $\Gamma_i = \Gamma$, $U_C = 0.3\Gamma$ and $\varepsilon = 0.3\Gamma$.

3 Conclusion

In this paper, we found that the four-terminal superconducting DQD has a topological singlet ground state with non-trivial topology in terms of the first Chern number C_{12} . This topological property could be in principle probed by measuring the transconductance when applying two voltages to terminals 1 and 2. As discussed in the manuscript, the topological phases exist in large parameter regions and are, thus, robust against fluctuations and noise.

We derived the effective single-particle Hamiltonian in the low energy limit and calculated its energy bands analytically. Introducing a many-body Hamiltonian allowed us to describe Coulomb repulsion between electrons on the same dot and determine the total spin of the ground state. We found that the topological phase can be maximized by choosing $\Gamma_i = \Gamma$ and $\varepsilon = \varepsilon_i = E_F = 0$. The non-trivial topology is preserved for finite Coulomb energy and magnetic field, but disappears when these quantities reach a critical value of about $\Gamma/2$.

We emphasize that this work discusses the relevant parameter regimes for which a quantized transconductance can be observed under experimentally realistic constraints of Coulomb interaction of a double quantum dot. Moreover, the proposed topological multiterminal junction lies within the reach of current or near term double quantum dot devices.

Acknowledgements

We acknowledge useful discussions with J. C. Cuevas.

Funding information This work was financially supported by the Deutsche Forschungsgemeinschaft (DFG; German Research Foundation) project no. 467596333 and project no. 425217212

via the Collaborative Research Center SFB 1432.

A Full Dyson equation and self-energy of the DQD

The full Dyson equation for the total system, consisting of the DQD and the four superconductors with coupling V can be written in matrix form as

$$\begin{pmatrix} \tilde{G}_{DD} & \tilde{G}_{DS} \\ \tilde{G}_{SD} & \tilde{G}_{SS} \end{pmatrix} = \begin{pmatrix} \tilde{g}_D & 0 \\ 0 & \tilde{g}_S \end{pmatrix} + \begin{pmatrix} \tilde{g}_D & 0 \\ 0 & \tilde{g}_S \end{pmatrix} \begin{pmatrix} 0 & \tilde{V}_{DS} \\ \tilde{V}_{DS}^\dagger & 0 \end{pmatrix} \begin{pmatrix} \tilde{G}_{DD} & \tilde{G}_{DS} \\ \tilde{G}_{SD} & \tilde{G}_{SS} \end{pmatrix}. \quad (\text{A1})$$

Plugging the equation for the G_{SD} component into the equation for G_{DD} , we obtain

$$\tilde{G}_{DD} = \tilde{g}_{DD} + \tilde{g}_{DD} \tilde{V}_{DS} \tilde{g}_{SS} \tilde{V}_{DS}^\dagger \tilde{G}_{DD}. \quad (\text{A2})$$

Comparing this with $\tilde{G}_{DD} = \tilde{g}_{DD} + \tilde{g}_{DD} \tilde{\Sigma}_{DD} \tilde{G}_{DD}$, yields the self-energy of the dot due to the dot-superconductor couplings, $\tilde{\Sigma}_{DD} = \tilde{V}_{DS} \tilde{g}_{SS} \tilde{V}_{DS}^\dagger$. Using the bare GF of the superconductors, $\tilde{g}_{S,j}(E) = -\pi N_0 e^{i\varphi_j \tau_3} \tau_1$ and the identity $\tau_3 \tau_1 \tau_3 = -\tau_1$, we get

$$\begin{aligned} \tilde{\Sigma}_{DD} &= \begin{pmatrix} w_0 & w_1 & 0 & 0 \\ 0 & 0 & w_2 & w_3 \end{pmatrix} \otimes \tau_3 \begin{pmatrix} \tilde{g}_{S,0} & 0 & 0 & 0 \\ 0 & \tilde{g}_{S,1} & 0 & 0 \\ 0 & 0 & \tilde{g}_{S,2} & 0 \\ 0 & 0 & 0 & \tilde{g}_{S,3} \end{pmatrix} \begin{pmatrix} w_0 & 0 \\ w_1 & 0 \\ 0 & w_2 \\ 0 & w_3 \end{pmatrix} \otimes \tau_3 \\ &= \begin{pmatrix} w_0^2 \tau_3 \tilde{g}_{S,0} \tau_3 + w_1^2 \tau_3 \tilde{g}_{S,1} \tau_3 & 0 \\ 0 & w_2^2 \tau_3 \tilde{g}_{S,2} \tau_3 + w_3^2 \tau_3 \tilde{g}_{S,3} \tau_3 \end{pmatrix} \\ &= \begin{pmatrix} 0 & \Gamma_0 + \Gamma_1 e^{i\varphi_1} & 0 & 0 \\ \Gamma_0 + \Gamma_1 e^{-i\varphi_1} & 0 & 0 & 0 \\ 0 & 0 & 0 & \Gamma_2 e^{i\varphi_2} + \Gamma_3 e^{i\varphi_3} \\ 0 & 0 & \Gamma_2 e^{-i\varphi_2} + \Gamma_3 e^{-i\varphi_3} & 0 \end{pmatrix}, \end{aligned} \quad (\text{A3})$$

with $\Gamma_j = \pi N_0 w_j^2$.

B Calculation of the many-body Hamiltonian

Choosing a basis B of many-body states, we obtain the matrix Hamiltonian \tilde{H} of a Hamiltonian H in second quantization by using twice the completeness relation $\sum_{\psi \in B} |\psi\rangle \langle \psi| = \mathbb{1}$ of the basis to obtain

$$H_{\text{MB}} = \sum_{\psi, \psi' \in B} |\psi\rangle \langle \psi| H |\psi'\rangle \langle \psi'|, \quad (\text{B1})$$

where the creation and annihilation operators in H naturally act on the many-body states in Fock space. It is, however, important to take into account the anticommutation relations of the fermionic operators and the antisymmetry of the fermionic Fock states when evaluating the matrix elements $\langle \psi| H |\psi'\rangle$.

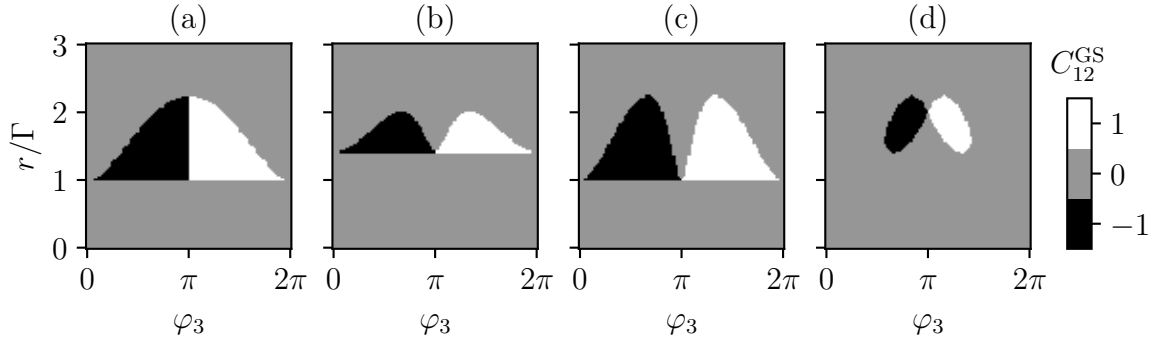


Figure 6: Topological phase diagrams for different sets of parameters. (a) for $\varepsilon_i = \varepsilon = \Gamma = \Gamma_i$. (b) for $\varepsilon_2 = 2\varepsilon_1 = \Gamma = \Gamma_i$. (c) for $\varepsilon_i = \varepsilon = \Gamma_0 = \Gamma_1$ and $\Gamma_2 = \Gamma_3 = 2\Gamma_0$. (d) for $\varepsilon_i = \varepsilon = \Gamma_0 = \Gamma_1 = \Gamma_2$ and $\Gamma_3 = 2\Gamma_0$.

C Effect of different parameters on the topological phase diagram

In Figure 6, the Chern number is shown as a function of φ_3 and r for symmetric parameters $\varepsilon_i = \varepsilon = \Gamma = \Gamma_i$ in (a), and in (b)-(d) for asymmetric parameters. The asymmetry leads to a deformation and separation of the topological phase in two regions but does not increase the area of the topological phase in respect of φ_3 and the inter-dot coupling r .

Figure 7 shows the topological phase diagram for different dot energies ε . The topological phase is clearly enhanced in the regime of weak inter-dot coupling r , especially in (d) for $\varepsilon = 0.1\Gamma \ll \Gamma$. This region is, however, not relevant for the observability of the topology.

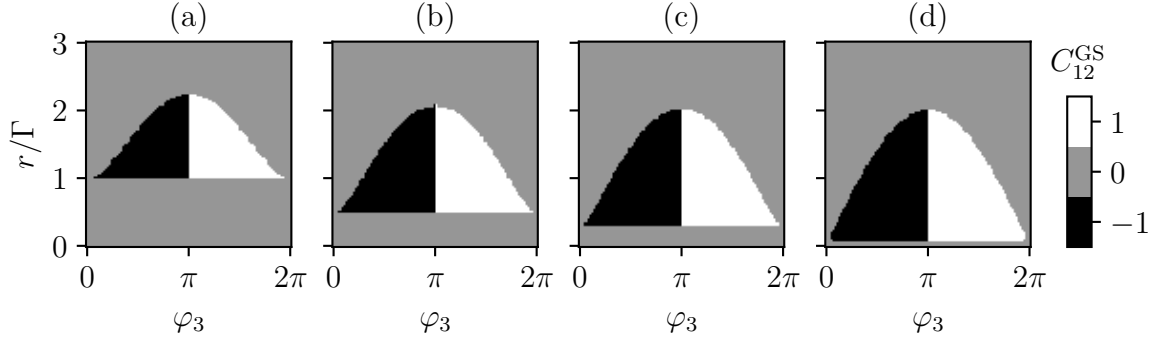


Figure 7: Topological phase diagrams for different quantum dot energies ε . In (a) for comparison $\varepsilon_i = \varepsilon = \Gamma = \Gamma_i$. (b) for $\varepsilon_i = \varepsilon = 0.5\Gamma = 0.5\Gamma_i$. (c) for $\varepsilon_i = \varepsilon = 0.3\Gamma = 0.3\Gamma_i$. (d) for $\varepsilon_i = \varepsilon = 0.1\Gamma = 0.1\Gamma_i$.

References

- [1] K. v. Klitzing, G. Dorda and M. Pepper, *New method for high-accuracy determination of the fine-structure constant based on quantized Hall resistance*, Phys. Rev. Lett. **45**(6), 494 (1980), doi:[10.1103/PhysRevLett.45.494](https://doi.org/10.1103/PhysRevLett.45.494).
- [2] Y. Hatsugai, *Chern number and edge states in the integer quantum Hall effect*, Phys. Rev. Lett. **71**(22), 3697 (1993), doi:[10.1103/PhysRevLett.71.3697](https://doi.org/10.1103/PhysRevLett.71.3697).
- [3] M. Z. Hasan and C. L. Kane, *Colloquium: topological insulators*, Rev. Mod. Phys. **82**(4), 3045 (2010), doi:[10.1103/RevModPhys.82.3045](https://doi.org/10.1103/RevModPhys.82.3045).
- [4] M. Sato and Y. Ando, *Topological superconductors: a review*, Rep. Prog. Phys. **80**(7), 076501 (2017), doi:[10.1088/1361-6633/aa6ac7](https://doi.org/10.1088/1361-6633/aa6ac7).
- [5] S. D. Sarma, M. Freedman and C. Nayak, *Majorana zero modes and topological quantum computation*, npj Quantum Inf. **1**(1), 1 (2015), doi:[10.1038/npjqi.2015.1](https://doi.org/10.1038/npjqi.2015.1).
- [6] M. Deng, S. Vaitiekėnas, E. B. Hansen, J. Danon, M. Leijnse, K. Flensberg, J. Nygård, P. Krogstrup and C. M. Marcus, *Majorana bound state in a coupled quantum-dot hybrid-nanowire system*, Science **354**(6319), 1557 (2016), doi:[10.1126/science.aaf3961](https://doi.org/10.1126/science.aaf3961).
- [7] D. Aasen, M. Hell, R. V. Mishmash, A. Higginbotham, J. Danon, M. Leijnse, T. S. Jespersen, J. A. Folk, C. M. Marcus, K. Flensberg and J. Alicea, *Milestones toward Majorana-based quantum computing*, Phys. Rev. X **6**(3), 031016 (2016), doi:[10.1103/PhysRevX.6.031016](https://doi.org/10.1103/PhysRevX.6.031016).
- [8] T. Karzig, C. Knapp, R. M. Lutchyn, P. Bonderson, M. B. Hastings, C. Nayak, J. Alicea, K. Flensberg, S. Plugge, Y. Oreg, C. M. Marcus and M. H. Freedman, *Scalable designs for quasiparticle-poisoning-protected topological quantum computation with Majorana zero modes*, Phys. Rev. B **95**(23), 235305 (2017), doi:[10.1103/PhysRevB.95.235305](https://doi.org/10.1103/PhysRevB.95.235305).
- [9] L. Lu, J. D. Joannopoulos and M. Soljačić, *Topological photonics*, Nat. Photon **8**(11), 821 (2014), doi:[10.1038/nphoton.2014.248](https://doi.org/10.1038/nphoton.2014.248).
- [10] T. Ozawa, H. M. Price, A. Amo, N. Goldman, M. Hafezi, L. Lu, M. C. Rechtsman, D. Schuster, J. Simon, O. Zilberberg *et al.*, *Topological photonics*, Rev. Mod. Phys. **91**(1), 015006 (2019), doi:[10.1103/RevModPhys.91.015006](https://doi.org/10.1103/RevModPhys.91.015006).
- [11] M. S. Rudner and N. H. Lindner, *Band structure engineering and non-equilibrium dynamics in Floquet topological insulators*, Nat. Rev. Phys. **2**(5), 229 (2020), doi:[10.1038/s42254-020-0170-z](https://doi.org/10.1038/s42254-020-0170-z).
- [12] S. Imhof, C. Berger, J. Bayer, F. Brehm, L. W. Molenkamp, T. Kiessling, F. Schindler, C. H. Lee, M. Greiter, T. Neupert *et al.*, *Topolectrical-circuit realization of topological corner modes*, Nat. Phys. **14**(9), 925 (2018), doi:[10.1038/s41567-018-0246-1](https://doi.org/10.1038/s41567-018-0246-1).
- [13] R.-P. Riwar, M. Houzet, J. S. Meyer and Y. V. Nazarov, *Multi-terminal Josephson junctions as topological matter*, Nature Commun. **7**(1), 1 (2016), doi:[10.1038/ncomms11167](https://doi.org/10.1038/ncomms11167).
- [14] E. Eriksson, R.-P. Riwar, M. Houzet, J. S. Meyer and Y. V. Nazarov, *Topological transconductance quantization in a four-terminal Josephson junction*, Phys. Rev. B **95**(7), 075417 (2017), doi:[10.1103/PhysRevB.95.075417](https://doi.org/10.1103/PhysRevB.95.075417).

- [15] H.-Y. Xie, M. G. Vavilov and A. Levchenko, *Topological Andreev bands in three-terminal Josephson junctions*, Phys. Rev. B **96**(16), 161406 (2017), doi:[10.1103/PhysRevB.96.161406](https://doi.org/10.1103/PhysRevB.96.161406).
- [16] H.-Y. Xie, M. G. Vavilov and A. Levchenko, *Weyl nodes in Andreev spectra of multiterminal Josephson junctions: Chern numbers, conductances, and supercurrents*, Phys. Rev. B **97**(3), 035443 (2018), doi:[10.1103/PhysRevB.97.035443](https://doi.org/10.1103/PhysRevB.97.035443).
- [17] O. Deb, K. Sengupta and D. Sen, *Josephson junctions of multiple superconducting wires*, Phys. Rev. B **97**(17), 174518 (2018), doi:[10.1103/PhysRevB.97.174518](https://doi.org/10.1103/PhysRevB.97.174518).
- [18] H.-Y. Xie and A. Levchenko, *Topological supercurrents interaction and fluctuations in the multiterminal Josephson effect*, Phys. Rev. B **99**(9), 094519 (2019), doi:[10.1103/PhysRevB.99.094519](https://doi.org/10.1103/PhysRevB.99.094519).
- [19] L. P. Gavensky, G. Usaj and C. A. Balseiro, *Topological phase diagram of a three-terminal Josephson junction: From the conventional to the Majorana regime*, Phys. Rev. B **100**(1), 014514 (2019), doi:[10.1103/PhysRevB.100.014514](https://doi.org/10.1103/PhysRevB.100.014514).
- [20] M. Houzet and J. S. Meyer, *Majorana-Weyl crossings in topological multiterminal junctions*, Phys. Rev. B **100**(1), 014521 (2019), doi:[10.1103/PhysRevB.100.014521](https://doi.org/10.1103/PhysRevB.100.014521).
- [21] R. L. Klees, G. Rastelli, J. C. Cuevas and W. Belzig, *Microwave Spectroscopy Reveals the Quantum Geometric Tensor of Topological Josephson Matter*, Phys. Rev. Lett. **124**, 197002 (2020), doi:[10.1103/PhysRevLett.124.197002](https://doi.org/10.1103/PhysRevLett.124.197002).
- [22] R. L. Klees, J. C. Cuevas, W. Belzig and G. Rastelli, *Ground-state quantum geometry in superconductor–quantum dot chains*, Phys. Rev. B **103**, 014516 (2021), doi:[10.1103/PhysRevB.103.014516](https://doi.org/10.1103/PhysRevB.103.014516).
- [23] I. Septembre, J. S. Meyer, D. D. Solnyshkov and G. Malpuech, *Weyl singularities in polaritonic multiterminal Josephson junctions*, Phys. Rev. B **107**, 165301 (2023), doi:[10.1103/PhysRevB.107.165301](https://doi.org/10.1103/PhysRevB.107.165301).
- [24] L. P. Gavensky, G. Usaj and C. A. Balseiro, *Multi-terminal Josephson junctions: A road to topological flux networks*, EPL **141**(3), 36001 (2023), doi:[10.1209/0295-5075/acb2f6](https://doi.org/10.1209/0295-5075/acb2f6).
- [25] R.-P. Riwar, *Fractional charges in conventional sequential electron tunneling*, Phys. Rev. B **100**(24), 245416 (2019), doi:[10.1103/PhysRevB.100.245416](https://doi.org/10.1103/PhysRevB.100.245416).
- [26] M. A. Javed, J. Schwibbert and R.-P. Riwar, *Fractional Josephson effect versus fractional charge in superconducting–normal metal hybrid circuits*, Phys. Rev. B **107**, 035408 (2023), doi:[10.1103/PhysRevB.107.035408](https://doi.org/10.1103/PhysRevB.107.035408).
- [27] V. Fatemi, A. R. Akhmerov and L. Bretheau, *Weyl Josephson circuits*, Phys. Rev. Research **3**(1), 013288 (2021), doi:[10.1103/PhysRevResearch.3.013288](https://doi.org/10.1103/PhysRevResearch.3.013288).
- [28] L. Peyruchat, J. Griesmar, J.-D. Pillet and Ç. Girit, *Transconductance quantization in a topological Josephson tunnel junction circuit*, Phys. Rev. Research **3**(1), 013289 (2021), doi:[10.1103/PhysRevResearch.3.013289](https://doi.org/10.1103/PhysRevResearch.3.013289).
- [29] T. Herrig and R.-P. Riwar, *Cooper-pair transistor as a minimal topological quantum circuit*, Phys. Rev. Research **4**, 013038 (2022), doi:[10.1103/PhysRevResearch.4.013038](https://doi.org/10.1103/PhysRevResearch.4.013038).

- [30] H. Weisbrich, R. L. Klees, G. Rastelli and W. Belzig, *Second Chern Number and Non-Abelian Berry Phase in Topological Superconducting Systems*, PRX Quantum **2**(1), 010310 (2021), doi:[10.1103/prxquantum.2.010310](https://doi.org/10.1103/prxquantum.2.010310).
- [31] H. Weisbrich, M. Bestler and W. Belzig, *Tensor Monopoles in superconducting systems*, Quantum **5**, 601 (2021), doi:[10.22331/q-2021-12-07-601](https://doi.org/10.22331/q-2021-12-07-601).
- [32] H.-Y. Xie, J. Hasan and A. Levchenko, *Non-Abelian monopoles in the multiterminal Josephson effect*, Phys. Rev. B **105**(24), L241404 (2022), doi:[10.1103/PhysRevB.105.L241404](https://doi.org/10.1103/PhysRevB.105.L241404).
- [33] C. Janvier, L. Tosi, Ç. Bretheau, L. and Girit, M. Stern, P. Bertet, P. Joyez, D. Vion, D. Esteve, M. F. Goffman, H. Pothier and C. Urbina, *Coherent manipulation of Andreev states in superconducting atomic contacts*, Science **349**(6253), 1199 (2015), doi:[10.1126/science.aab2179](https://doi.org/10.1126/science.aab2179).
- [34] D. J. Van Woerkom, A. Proutski, B. Van Heck, D. Bouman, J. I. Väyrynen, L. I. Glazman, J. Krogstrup, Pand Nygård, L. P. Kouwenhoven and A. Geresdi, *Microwave spectroscopy of spinful Andreev bound states in ballistic semiconductor Josephson junctions*, Nat. Phys. **13**(9), 876 (2017), doi:[10.1038/nphys4150](https://doi.org/10.1038/nphys4150).
- [35] M. Hays, G. De Lange, D. J. Serniak, K. and Van Woerkom, D. Bouman, P. Krogstrup, J. Nygård, A. Geresdi and M. H. Devoret, *Direct microwave measurement of Andreev-bound-state dynamics in a semiconductor-nanowire Josephson junction*, Phys. Rev. Lett. **121**(4), 047001 (2018), doi:[10.1103/PhysRevLett.121.047001](https://doi.org/10.1103/PhysRevLett.121.047001).
- [36] J. D. Pillet, C. H. L. Quay, P. Morfin, C. Bena, A. L. Yeyati and P. Joyez, *Andreev bound states in supercurrent-carrying carbon nanotubes revealed*, Nat. Phys. **6**(12), 965 (2010), doi:[10.1038/nphys1811](https://doi.org/10.1038/nphys1811).
- [37] L. Bretheau, Ç. Girit, C. Urbina, D. Esteve and H. Pothier, *Supercurrent spectroscopy of Andreev states*, Phys. Rev. X **3**(4), 041034 (2013), doi:[10.1103/PhysRevX.3.041034](https://doi.org/10.1103/PhysRevX.3.041034).
- [38] A. W. Draelos, M.-T. Wei, A. Serebinski, H. Li, Y. Mehta, K. Watanabe, T. Taniguchi, I. V. Borzenets, F. Amet and G. Finkelstein, *Supercurrent flow in multiterminal graphene Josephson junctions*, Nano Lett. **19**(2), 1039 (2019), doi:[10.1021/acs.nanolett.8b04330](https://doi.org/10.1021/acs.nanolett.8b04330).
- [39] N. Pankratova, R. Lee, H. and Kuzmin, K. Wickramasinghe, W. Mayer, J. Yuan, M. G. Vavilov, J. Shabani and V. E. Manucharyan, *Multiterminal Josephson effect*, Phys. Rev. X **10**(3), 031051 (2020), doi:[10.1103/PhysRevX.10.031051](https://doi.org/10.1103/PhysRevX.10.031051).
- [40] E. G. Arnault, T. F. Q. Larson, A. Serebinski, L. Zhao, S. Idris, A. McConnell, K. Watanabe, T. Taniguchi, I. Borzenets, F. Amet *et al.*, *Multiterminal inverse ac Josephson effect*, Nano Lett. **21**(22), 9668 (2021), doi:[10.1021/acs.nanolett.1c03474](https://doi.org/10.1021/acs.nanolett.1c03474).
- [41] M. Coraiola, D. Z. Haxell, D. Sabonis, H. Weisbrich, A. E. Svetogorov, M. Hinderling, S. C. ten Kate, E. Cheah, F. Krizek, R. Schott, W. Wegscheider, J. C. Cuevas *et al.*, *Hybridisation of Andreev bound states in three-terminal Josephson junctions*, arXiv preprint arXiv:2302.14535 (2023), doi:[10.48550/arXiv.2302.14535](https://doi.org/10.48550/arXiv.2302.14535), ArXiv:2302.14535.
- [42] M. Kocsis, Z. Scherübl, G. Fülöp, P. Makk and C. S., *Strong nonlocal tuning of the current-phase relation of a quantum dot based Andreev molecule*, arXiv preprint arXiv:2303.14842 (2023), doi:[10.48550/arXiv.2303.14842](https://doi.org/10.48550/arXiv.2303.14842), ArXiv:2303.14842.

- [43] O. Kurtossy, Z. Scherübl, G. Fülöp, I. E. Lukács, T. Kanne, J. Nygård, P. Makk and S. Csonka, *Andreev molecule in parallel InAs nanowires*, Nano Lett. **21**(19), 7929 (2021), doi:[10.1021/acs.nanolett.1c01956](https://doi.org/10.1021/acs.nanolett.1c01956).
- [44] O. Kurtossy, Z. Scherübl, G. Fülöp, I. E. Lukács, T. Kanne, J. Nygård, P. Makk and S. Csonka, *Parallel InAs nanowires for Cooper pair splitters with Coulomb repulsion*, npj Quantum Mater. **7**(1), 88 (2022), doi:[10.1038/s41535-022-00497-9](https://doi.org/10.1038/s41535-022-00497-9).
- [45] J. Gramich, A. Baumgartner and C. Schönenberger, *Andreev bound states probed in three-terminal quantum dots*, Phys. Rev. B **96**(19), 195418 (2017), doi:[10.1103/PhysRevB.96.195418](https://doi.org/10.1103/PhysRevB.96.195418).